Journal of Mathematical Neuroscience (0) 0
The Journal of Mathematical Neuroscience
a SpringerOpen Journal
RESEARCH Open Access

Modelling Calcium Waves in Different Dendritic Structures

Ana Victoria Ponce Bobadilla · Yulia Timofeeva

Abstract Calcium plays an important role in regulating a great variety of neuronal processes. Here we propose an analytically tractable spatiotemporal model of dendritic calcium concentration. We take into account two sources of Ca^{2+} : voltage-gated calcium channels (VGCCs) on the dendritic membrane and ryanodine receptors (RyRs) on the surface membrane of the endoplasmic reticulum. We investigate how the cell geometry and the distribution of VGCCs and RyRs affect the generation and propagation of Ca^{2+} waves. Mimicking the nonlinear behaviour of the RyRs and the VGCCs using threshold processes, the model results in a system of coupled piecewise partial differential equations which are solved in terms of the appropriate Green's function given the domain and the boundary conditions. The model is considered in two simplified dendritic structures where we analyze the critical conditions in the parameter space at which a calcium wave either propagates or does not and at which a wave may or may not enter the soma. We analyze the situation in which one VGCC is activated as initial condition. In this case, we show how the presence of soma affects the Ca^{2+} dynamics. Furthermore, we find the existence of a critical diameter size of the soma (a_S^*) below which the calcium wave fails to initiate and above which, the calcium wave initiates and reaches the soma. To obtain insight into a_S^*, we analyze the behaviour of the models for different diameters of the soma, and we determine how the critical diameter size changes with respect to the distance from the initially activated VGCC to the soma. Finally, we analyze the dependence of the calcium wave on the density of the RyRs.

Keywords dendrites · calcium waves · ryanodine receptor · fire-diffuse-fire model · spike-diffuse-spike model

List of Abbreviations
RyR: Ryanodine receptor
VGCC: Voltage-gated calcium channel
CICR: Ca^{2+}-induced Ca^{2+} release mechanism
ER: Endoplasmic Reticulum
IP_3R: Inositol (1,4,5)-trisphosphate receptors

Ana Victoria Ponce Bobadilla
Centre for Complexity Science, University of Warwick, Coventry, CV4 7AL, UK
e-mail: anavictoria.ponce@gmail.com

Yulia Timofeeva
Department of Computer Science and Centre for Complexity Science, University of Warwick, Coventry, CV4 7AL, UK
e-mail: y.timofeeva@warwick.ac.uk

1 Introduction

Intracellular calcium (Ca^{2+}) signals regulate numerous cellular processes: cell differentiation, gene transcription, fertilization, cell proliferation and many others [3]. Changes in [Ca^{2+}] do not occur uniformly throughout the cell but are initiated at a specific site and they spread in the form of intracellular waves [21]. Neurons present widespread Ca^{2+} signals and spark events (spontaneously localized Ca^{2+} release events)[15]. The variety of neuronal cell types and their complex branching structures lead to diverse calcium patterns which have not yet been rigorously studied [15].

The most characterizing change in Ca^{2+} concentration in neurons is generated from the opening of voltage-gated calcium channels (VGCCs) [15]. At resting membrane potential, VGCCs are closed; when the neuron depolarizes the channels open and rush Ca^{2+} into the cell [22]. Ca^{2+} signals triggered by internal stores are less well studied in neurons [15]. In the past, this kind of signals were not studied since they were not directly associated with the membrane potential and detecting them in the dendrites was very difficult. However, with the existence of more sensitive Ca^{2+} indicators and pharmacological and immunochemical evidence that calcium changes from internal stores are significant there is a renewed interest in the study of these signals [15].

Internal calcium sources are located in the endoplasmic reticulum (ER) or its equivalent in muscle cells, sarcoplasmic reticulum [3]. The ER extends continuosly through the dendrites of piramidal neurons and Purkinje neurons [17, 11]. Influx from these internal stores is controlled by various channels: the inositol (1,4,5)-trisphosphate receptors (IP_3Rs) and the ryanodine receptors (RyRs). In this work, we will focus only on the RyRs. The activation of these receptors is through a process called Ca^{2+} - induced Ca^{2+} release (CICR). In this mechanism elevated cytoplasmic Ca^{2+} induces the activation of the RyRs and a release of further Ca^{2+} . The released Ca^{2+} acts on nearby RyRs to release more Ca^{2+} and this chain continues if the density of Ca^{2+} channels and Ca^{2+} concentration are suitable.

Analyzing whether the calcium wave reaches the soma is relevant since it has been suggested that Ca^{2+} waves carry information from a synapse in the dendrite to the nucleus where the large concentration of Ca^{2+} could activate genes or transcription factors involved in synaptic plasticity [14, 8]. Experimentally, it has been observed that some synaptic stimulation in hippocampal slices generates Ca^{2+} waves confined to dendrites [14]. These waves rarely reach the soma because there are few synaptic contacts in this region, however the presence of enough RyRs (or IP_3Rs) can allow waves to spread into the soma. When this happens, an intense Ca^{2+} release is generated in the cell body and nucleus due to the high concentration of IP_3Rs and RyRs in the soma and nuclear membrane [14].

The distribution of the RyRs are vitally important for determining whether Ca^{2+} release transforms into a propagating Ca^{2+} wave. Just taking into account the internal stores, the waves will spread as far as RyR are available and in sufficient densities to support CICR. Since the molecular configuration is distinctive for different regions of the cell and for particular neuronal cell types, distributions of receptors and channels vary in neurons [4] which means that analyzing the calcium wave's dependence on the distribution of the receptors is relevant.

The goal of this paper is to investigate how the cell geometry and the distribution of VGCCs and RyRs affect the generation and propagation of Ca^{2+} waves. We will consider a system of coupled partial differential equations to model the voltage and the calcium dynamics. In order to analyze the influence of the cell geometry, we will consider two different dendritic structures: an infinite cable and a semi-infinite cable with a lumped soma. We will analyze the effects of the presence and size of the soma by considering the two models and varying the soma's diameter. To analyze the distribution we will consider a uniform distribution of VGCCs and consider a fixed amount of RyRs between them, varying this amoun to see its impact on calcium dynamics.

The structure of the paper is as follows: in Section 2 we introduce the equations for the infinite cable and semi-infinite cable with lumped soma and prove the existence of solutions. In Section 3.1, we analyze the effect of soma's presence. We also analyze the influence of its size by varying the diameter and recording the spiking times and the voltage and calcium profiles in different positions. In Section 3.2, we analyze the effects of different meshes in the calcium dynamics. In Section 4, we describe other features that the model could take into account and some limitations of the model. Finally, in this section, we give the main conclusions from the research.

2 Model

We propose a model that integrates the voltage and the calcium dynamics in the dendrite. We consider a passive dendrite cable with a distribution of VGCCs along its length L. The dynamics of the membrane voltage in the cable ($V = V(x,t)$) are described by the well known cable equation

$$\pi a C_m \frac{\partial V}{\partial t} = -\frac{\pi a V}{R_m} + \frac{\pi a^2}{4R_a}\frac{\partial^2 V}{\partial x^2} + \rho(x)I(t), \tag{1}$$

where a is the diameter of the cable (measured in μm), R_a is the specific cytoplasmic resistivity (in Ω·cm), C_m is the specific membrane capacity (in $\mu F/cm^2$) and R_m is the resistance across a unit area of a passive membrane (in Ω/cm^2).

The VGCCs are located at discrete points x_n determined by a distribution function $\rho(x) = \sum_{n\in\Gamma}\delta(x - x_n)$, where Γ is a discrete set that indexes the VGCCs. The VGCCs generate current described by the profile function $I(t) = \eta_V(t - T_V(x_n))$, where $T_V(x_n)$ denotes a firing time for the VGCC in the location x_n. The time $T_V(x_n)$ is defined as follows,

$$T_V(x_n) = \inf\left\{ t \mid V(x_n,t) > h_{V_{th}},\ \frac{\partial V(x,t)}{\partial t} > 0 \right\}.$$

By this definition, once $V(x_n,t)$ crosses a certain threshold value $h_{V_{th}}$, the VGCC fires. If we only allow each VGCC to fire once, the behaviour mimics a long-lasting refractory state.

Equation (1) can be rewritten as

$$\frac{\partial V}{\partial t} = -\frac{V}{\tau_V} + D_V\frac{\partial^2 V}{\partial x^2} + \sum_n \delta(x - x_n)\eta_V(t - T_V(x_n)),$$

where $D_V = a/4R_aC_m$ (in $\mu m^2/ms$) denotes the diffusion coefficient of the cable and $\tau_V = C_mR_m$ (in ms) is the membrane time constant. This is the spike-diffuse-spike model, one of the typical models for describing voltage dynamics[5].

For calcium dynamics we consider a similar model for CICR, the so called "fire- diffuse-fire model" introduced by Keizer [9]. In a similar fashion as the previous model, the RyRs are located at discrete points y_i. There is an instantaneous release of a fixed amount σ_C of Ca^{2+} when $C(x,t)$ exceeds a threshold value $h_{C_{th}}$. After the release, the site becomes refractory. In addition, the released calcium diffuses and may trigger another instantaneous release (spark) at neighboring sites.

To include the effect of the VGCCs in the calcium dynamics, we take into account the term $\sum_n \delta(x-x_n)\eta_V(t-T_V(x_n))$ from the voltage dynamics and multiply it by a conversion factor γ_C to change calcium current to calcium concentration. The final model is the following:

$$\begin{cases} \frac{\partial V}{\partial t} = -\frac{V}{\tau_V} + D_V\frac{\partial^2 V}{\partial x^2} + \sum\limits_n \delta(x-x_n)\eta_V(t-T_V(x_n)), \\ \frac{\partial C}{\partial t} = -\frac{C}{\tau_C} + D_C\frac{\partial^2 V}{\partial x^2} + \gamma_C\sum\limits_n \delta(x-x_n)\eta_V(t-T_V(x_n)) + \sum\limits_i \delta(x-y_i)\eta_C(t-T_C(y_i)), \end{cases} \tag{2}$$

where

$$T_V(x_n) = \inf\left\{ t \mid V(x_n,t) > h_{V_{th}},\ \frac{\partial V(x_n,t)}{\partial t} > 0 \right\},$$

$$T_C(y_i) = \inf\left\{ t \mid C(y_i,t) > h_{C_{th}},\ \frac{\partial C(y_i,t)}{\partial t} > 0 \right\},$$

and the profile functions are rectangular pulses

$$\eta_V(t) = \sigma_V\theta(t)\theta(\tau_{R_V}-t) \quad \text{and} \quad \eta_C(t) = \sigma_C\theta(t)\theta(\tau_{R_C}-t),$$

in which σ_V is the strength of the pulse and τ_{R_V} is its duration (similarly for σ_C and τ_{R_C}).

We now consider two domains for this model: an infinite cable and a semi-infinite cable with lumped soma. In the next subsections we prove the existence of a solution to (2) in these domains.

2.1 Infinite cable

Consider the real line as the space domain, zero initial conditions and the following boundary conditions,

$$V(\pm\infty,t) < \infty \quad \text{and} \quad C(\pm\infty,t) < \infty.$$

We have the following result:

Theorem 1 (Existence of a solution for the infinite cable)**.** *For the PDE model* (2) *with zero initial and the above boundary conditions, there exists a solution given by,*

$$V(x,t) = \sigma_V \sum_n H_V(x, x_n, t - T_V(x_n)) \tag{3}$$

$$C(x,t) = \gamma_C \sigma_V \sum_n H_C(x, x_n, t - T_V(x_n)) + \sigma_C \sum_i H_C(x, y_i, t - T_C(y_i)), \tag{4}$$

where

$$H_N(x, x_0, t) = A(x - x_0, t - min(t, \tau_{R_N})) - A(x - x_0, t),$$

in which

$$A(x,t) = \frac{1}{4\sqrt{\epsilon_N D_N}} \left\{ \exp\left(-|x| \sqrt{\frac{\epsilon_N}{D_N}}\right) \operatorname{erfc}\left(-\frac{|x|}{\sqrt{4D_N t}} + \sqrt{\epsilon_N t}\right) + \exp\left(|x| \sqrt{\frac{\epsilon_N}{D_N}}\right) \operatorname{erfc}\left(\frac{x}{4D_N t} + \sqrt{\epsilon_N t}\right) \right\}$$

with $\epsilon_N = \frac{1}{\tau_{R_N}}$ *and* $N = V$ *or* C *for the VGCCs and RyRs respectively.*

Proof. First we consider the following equation

$$\frac{\partial H}{\partial t} = -\frac{H}{\tau} + D\frac{\partial^2 H}{\partial x^2} + \eta(t)\delta(x - x_0), \tag{5}$$

where $\eta(t) = \sigma_0 \theta(t)\theta(\tau_R - t)$.

In order to solve (5), we consider the Fourier transform of this function with respect to space ($x \to \kappa$), then (5) turns into

$$\widetilde{H}_t = -D\kappa^2 \widetilde{H} - \epsilon \widetilde{H} + \eta(t) e^{-i\kappa x_0}.$$

This can be rewritten as

$$\widetilde{H}_t = -\sigma(\kappa)\widetilde{H} + \eta(t) e^{-i\kappa x_0},$$

where $\sigma(\kappa) = D\kappa^2 + \epsilon$.

By solving this ODE, we get

$$\widetilde{H} e^{\sigma(\kappa)t} = \int_0^t \eta(s) e^{-i\kappa x_0} e^{\sigma(\kappa)s} ds.$$

Recalling that $\eta(t) = \sigma_0 \theta(t)\theta(\tau_R - t)$, we have

$$\widetilde{H} e^{\sigma(\kappa)t} = \sigma_0 \int_0^{\min(t,\tau_R)} e^{-i\kappa x_0} e^{\sigma(\kappa)s} ds,$$

where we get

$$\widetilde{H} e^{\sigma(\kappa)t} = \sigma_0 \frac{e^{-i\kappa x_0} e^{\sigma(\kappa)s}}{\sigma(\kappa)} \Bigg|_0^{\min(t,\tau_R)} = \eta_0 \frac{e^{-i\kappa x_0} e^{\sigma(\kappa)\min(t,\tau_R)} - e^{-i\kappa x_0}}{\sigma(\kappa)}.$$

Then we have

$$\widetilde{H}(\kappa,t)=\sigma_0\frac{e^{-i\kappa x_0}e^{-\sigma(\kappa)(t-\min(t,\tau_R))}}{\sigma(\kappa)}-\sigma_0\frac{e^{-i\kappa x_0}e^{-\sigma(\kappa)t}}{\sigma(\kappa)}.$$

Taking the inverse Fourier transform, we introduce the function

$$A(x,t)=\int_{-\infty}^{\infty}\frac{d\kappa}{2\pi}\frac{e^{-\sigma(\kappa)t}e^{i\kappa x}}{\sigma(\kappa)}. \tag{6}$$

Then the solution is given by

$$H(x,x_0,t)=\sigma_0\left[A(x-x_0,t-\min(t,\tau))-A(x-x_0,t)\right].$$

A closed form for the integral is given explicitly in [7] by

$$A(x,t)=\frac{1}{4\sqrt{\epsilon_N D_N}}\left\{\exp\left(-|x|\sqrt{\frac{\epsilon_N}{D_N}}\right)\operatorname{erfc}\left(-\frac{|x|}{\sqrt{4D_N t}}+\sqrt{\epsilon_N t}\right)\right.$$
$$\left.+\exp\left(|x|\sqrt{\frac{\epsilon_N}{D_N}}\right)\operatorname{erfc}\left(\frac{x}{4D_N t}+\sqrt{\epsilon_N t}\right)\right\}.$$

Following the previous approach for each of the terms in $\sum_n \delta(x-x_n)\eta_V(t-T_V(x_n))$ in (2) and noticing that (2) is a system of piecewise linear PDEs, then the solution for $V(x,t)$ is given by a linear combination of the solutions defined by the terms $\delta(x-x_n)\eta_V(t-T_V(x_n))$ (with the previous approach) and therefore the solution for $V(x,t)$ in (2) takes the form of (3). We can perform analogous approach for the terms in $\sum_i \delta(x-y_i)\eta_C(t-T_V(y_i))$ to prove that $C(x,t)$ takes the form (4) as desired. □

2.2 Semi-infinite cable with lumped soma

Consider equation (2) on the semi-infinite positive real line with a lumped soma at $x=0$. This situation gives the following somatic boundary conditions in the origin

$$|V(\infty,t)|<\infty \quad \text{and} \quad g_S V(0,t)+C_S\frac{\partial V(0,t)}{\partial t}-\frac{1}{r_m}\frac{\partial V(x,t)}{\partial x}\bigg|_{x=0}=0,$$

$$|C(\infty,t)|<\infty \quad \text{and} \quad C(0,t)+\tau_C\frac{\partial C(0,t)}{\partial t}-\left(\frac{D_C\tau_C a}{a_S^2}\right)\frac{\partial C(x,t)}{\partial x}\bigg|_{x=0}=0,$$

where a_S (in μm) is the diameter of the soma, $g_S=\pi a_S^2 R_m$ and $C_S=\pi a_S^2 C_m$ are the conductance and capacitance of the soma respectively, $r_m=4R_a/\pi a^2$ (Ω/cm) is the axial resistance along the dendrite. The form of the boundary condition for this structure is explained in [20].

We have the following result:

Theorem 2 (Existence of a solution for the semi-infinite cable with lumped soma). *Considering zero initial boundary conditions and the somatic boundary conditions above, then* (2) *has a solution given by*

$$V(x,t) = \sigma_V \sum_{n,m} \widehat{H}_C(x, x_n, t - T_V^m(x_n)) \tag{7}$$

$$C(x,t) = \gamma_C \sigma_V \sum_{n,m} \widehat{H}_C(x, x_n, t - T_V^m(x_n)) + \sigma_C \sum_{i,j} \widehat{H}_C(x, y_i, t - T_C^j(y_i)), \tag{8}$$

where

$$\widehat{H}_V(x, x_0, t) = B(x, x_0, t) - B(x, x_0, t - \tau_{R_N}),$$

and

$$B(x,y,t) = \frac{1}{4}\sqrt{\frac{\tau_N}{D_N}}\left[f_{-1}(x-y,t) - f_1(x-y,t) + \frac{\alpha-1}{\alpha+1}f_{-1}(x-y,t)\right.$$
$$\left. - \frac{\alpha+1}{\alpha-1}f_1(x+y,t) + \frac{4\alpha}{\alpha^2-1}f_\alpha(x+y,t)\right],$$

where $\alpha = \frac{a}{a_S^2}\sqrt{\tau_N D_N}$ *and*

$$f_a(x,t) = \exp\left(\frac{a|x|}{\sqrt{\tau_N D_N}} + \frac{(a^2-1)t}{\tau_N}\right)\operatorname{erfc}\left(\frac{|x|}{\sqrt{4D_N t}} + a\sqrt{\frac{t}{\tau_N}}\right),$$

and $N = V$ *and* C *for the VGCC and RyRs respectively.*

Proof. In a similar way as for the infinite cable, we consider first the following PDE:

$$\frac{\partial \overline{H}}{\partial t} = -\frac{\overline{H}}{\tau_V} + D\frac{\partial^2 \overline{H}}{\partial x^2} + \eta(t)\delta(x - x_0), \tag{9}$$

where $\eta_V(t) = \sigma_V \theta(t)\theta(\tau_{R_V} - t)$ and the boundary conditions

$$|\overline{H}(\infty, t)| < \infty \quad \text{and} \quad g_S \overline{H}(0,t) + C_S \frac{\partial \overline{H}(0,t)}{\partial t} - \frac{1}{r_m}\frac{\partial \overline{H}(x,t)}{\partial x}\bigg|_{x=0} = 0.$$

In this case we consider the voltage parameters but an analogous result can be obtain for the calcium parameters.

Since equation (9) is a linear PDE, the solution can be explicitly obtained by

$$\overline{H}(x,t) = \int_0^t G(x, y, t-s)\eta_V(s)ds, \tag{10}$$

where G is the Green's function of the domain with the boundary conditions.

Applying a Laplace transform in time $\mathcal{L}(t \to \omega)$ to (10) we get

$$\mathcal{L}(\overline{H}) = \mathcal{L}(G)(x, y, \omega) \cdot \mathcal{L}(\eta)(\omega),$$

since it is the Laplace transform of a convolution [2].

The Green function of the domain with the boundary conditions in the Laplace domain is given in [19] and is the following

$$\mathcal{L}(G)(x,y,s) = (2p(\omega)-1)\frac{e^{-|x+y|\gamma(\omega)}}{2D_V\gamma(\omega)} + \frac{e^{-|x-y|\gamma(\omega)}}{2D_V\gamma(\omega)},$$

where $p(\omega) = \frac{\gamma(\omega)}{\gamma(\omega)+r_m\gamma_S(\omega)}$, $\gamma^2(\omega) = (\omega + 1/\tau_V)/D_V$ and $\gamma_S(\omega) = C_S(\omega) + g_S$.

Applying a Laplace transform to $\eta_V(t)$, we get

$$\mathcal{L}(\eta_V)(\omega) = \frac{\sigma_V}{\omega}(1 - e^{-\omega\tau_{R_V}}).$$

After some algebraic manipulation, we have that

$$\mathcal{L}(\overline{H})(x,y,\omega) = \mathcal{L}(G)(x,y,\omega)\cdot\mathcal{L}(\eta_V)(\omega) = \sigma_V\left[\mathcal{L}(B)(x,y,\omega) - e^{-\omega\tau_{R_V}}\mathcal{L}(B)(x,y,\omega)\right],$$

where

$$\mathcal{L}(B)(x,y,\omega) = \mathcal{L}(A)(x-y,\omega) - \mathcal{L}(A)(x+y,\omega) + \mathcal{L}(P)(x+y,\omega),$$

$$\mathcal{L}(A)(x,\omega) = \frac{2D_V e^{-|x|\gamma(\omega)}}{\omega\gamma(\omega)},$$

$$\mathcal{L}(P)(x,\omega) = \frac{D_V e^{-|x|\gamma(\omega)}\gamma(\omega)}{\omega(\gamma(\omega)+r\gamma_S(\omega))}.$$

From [6] we know that

$$A(x,t) = \mathcal{L}^{-1}\mathcal{L}(A)(x,\omega) = \frac{\sqrt{\tau_V}}{4\sqrt{D_V}}\left\{\exp\left(-|x|\sqrt{\frac{\epsilon_V}{D_V}}\right)\operatorname{erfc}\left(-\frac{|x|}{\sqrt{4D_Vt}} + \sqrt{\epsilon_V t}\right)\right.$$
$$\left. + \exp\left(|x|\sqrt{\frac{\epsilon_V}{D_V}}\right)\operatorname{erfc}\left(\frac{x}{4D_Vt} + \sqrt{\epsilon_V t}\right)\right\}.$$

Using $\omega = D_V\gamma^2 - \epsilon_V$, $\epsilon_V = 1/\tau_V$ and $g_S = C_S\epsilon_V$, we have

$$\mathcal{L}(P)(x,\omega) = \exp(-|x|\gamma)\frac{\epsilon\alpha}{D_V^2\gamma(\gamma^2-\epsilon/D_V)(\gamma+\alpha\sqrt{\epsilon/D_V})}, \tag{11}$$

in which $\alpha = \frac{a}{a_S^2}\sqrt{\tau_V D_V}$.

Using partial fractions, we have

$$\mathcal{L}(P)(x,\omega) = \frac{\alpha}{2\sqrt{\epsilon}(\alpha^2-1)}\exp\left(-|x|\sqrt{\frac{\omega+\epsilon}{D_V}}\right)\left[\frac{\alpha-1}{\sqrt{\omega+\epsilon}-\sqrt{\epsilon}} + \frac{\alpha+1}{\sqrt{\omega+\epsilon}+\sqrt{\epsilon}}\right.$$
$$\left. - \frac{2}{\alpha}\frac{1}{\sqrt{\omega+\epsilon}+\alpha\sqrt{\epsilon}} - \frac{1}{\sqrt{\omega+\epsilon}}\right].$$

Performing the inverse Laplace transform $P(x,t) = \mathcal{L}^{-1}[\mathcal{L}(P)(x,\omega)]$ and using the inverse Laplace relationships (which can be found in [2]), we have

$$\mathcal{L}^{-1}[\mathcal{L}(f)(\omega+\epsilon)] = e^{-\epsilon t}\mathcal{L}^{-1}[\mathcal{L}(f)(\omega)],$$

and

$$\mathcal{L}^{-1}\left[\frac{e^{-|x|\sqrt{\omega}}}{\sqrt{\omega}+a}\right] = \frac{1}{\sqrt{\pi t}}e^{-\frac{x^2}{4t}} - ae^{a|x|}e^{a^2t}\operatorname{erfc}\left(a\sqrt{t}+\frac{|x|}{2\sqrt{t}}\right),$$

we get

$$P(x,t) = \frac{\tau_V}{D_V}\left[\frac{\alpha}{2(\alpha+1)}f_{-1}(x,t) - \frac{\alpha}{2(\alpha-1)}f_1(x,t) + \frac{\alpha}{\alpha^2-1}f_\alpha(x,t)\right]$$

where

$$f_a(x,t) = \exp\left(\frac{a|x|}{\sqrt{\tau_V D_V}} + \frac{(a^2-1)t}{\tau_V}\right)\operatorname{erfc}\left(\frac{|x|}{\sqrt{4D_V t}} + a\sqrt{\frac{t}{\tau_V}}\right)$$

□

Following the previous approach for each of the terms in $\sum_n \delta(x-x_n)\eta_V(t-T_V(x_n))$ in (2) and noticing that (2) is a system of piecewise linear PDEs, then the solution for $V(x,t)$ is given by a linear combination of the solutions defined by the terms $\delta(x-x_n)\eta_V(t-T_V(x_n))$ (with the previous approach) and therefore the solution for $V(x,t)$ in (2) takes the form of (7). We can perform analogous approach for the terms in $\sum_i \delta(x-y_i)\eta_C(t-T_V(y_i))$ to prove that $C(x,t)$ takes the form (8) as desired.

3 Results

3.1 Soma's influence in the overall dynamics

To analyze the effect of the soma's presence, we perform simulations considering the same parameters for voltage and calcium in the infinite cable and the semi-infinite cable with a lumped soma. The parameters are described in Appendix A. For both situations we consider a dendrite of length 40 μm and an uniform density of VGCCs located at a fixed distance and three RyR between each pair of VGCCs. For initial conditions we take both calcium and voltage equal to zero and we consider that the last VGCC in our mesh is activated. This can be thought of as an injection of current at that location.

Influence of the soma's presence

Considering a soma with diameter 25μm in the semi-infinite cable with lumped soma, a calcium wave is formed. On the other hand, in the infinite cable there is no calcium wave. In both models the activation of the last VGCC makes all the VGCCs to fire. In Figure 1, space-time diagrams of calcium concentration is plotted for both models. For each time, the concentration is plotted at each position along the dendrite. The small sparks close to the x-axis are the influx from the VGCCs which are present in both models. In the semi-infinite cable with lumped soma case the calcium wave is initiated from the second-to-last RyR and the wave continues until it reaches the soma in between 2.5-3 s.

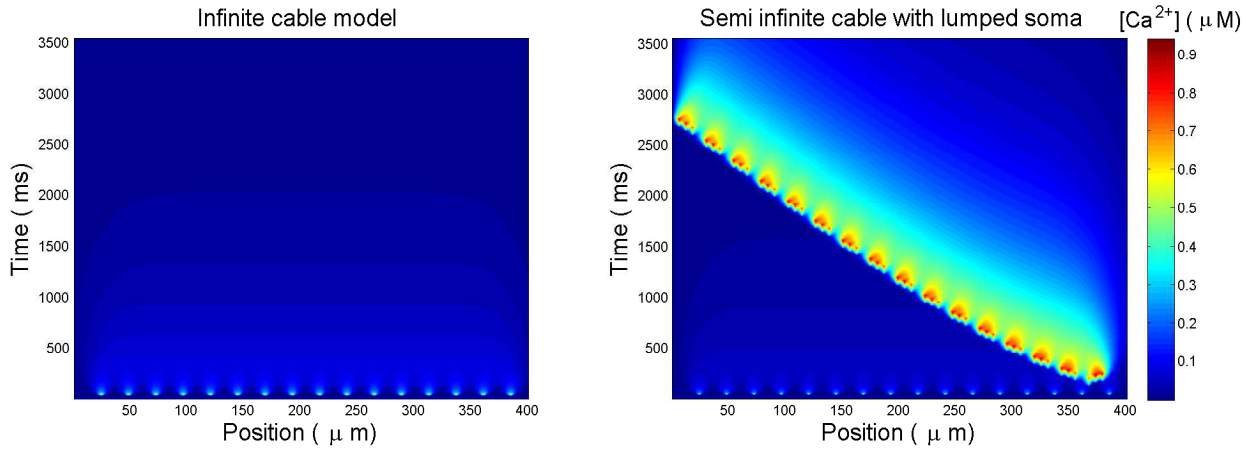

Figure 1: Calcium concentration in the two models. The solution for the dendrite is plotted for each time step. In the semi-infnite cable with lumped soma, there is a calcium wave that propagates. This illustrates the influence of the soma's presence. (Simulation parameters are give in Appendix A and $a_S = 25\mu$m)

Influence of the soma's size

Varying the diameter of the soma, it is seen that there is a critical value for the diameter $a_S^* \approx 22.81$. Below a_S^* the wave fails to propagate and above it the calcium wave initiates and reaches the soma. This can be seen in Figure 2, where we plot the reaching times for the calcium wave to reach the soma for different diameter sizes.

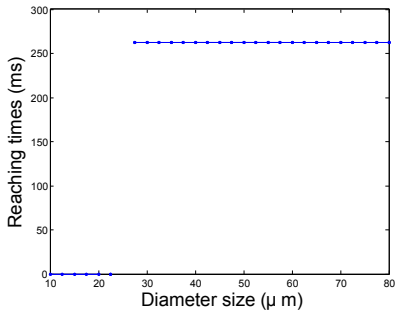

Figure 2: Reaching times for the calcium wave to reach the soma for different diameter size. The graph shows the critical diameter size below which the calcium waves fails to exist and above which reaches the soma.

First we analyze the different behaviours of the dynamics while varying the soma's diameter. One feature that is present in both models is the spiking of all VGCCs. We record the spiking time for each VGCC for the infinite cable model and for the semi-infinite cable with lumped soma model with diameter values $a_S = 20, 30$ and 40 μm. As can be seen in Figure 3 (A) as we increase the soma's diameter, the spiking time of the VGCCs increase. Also for $a_S = 30$ and 40μm the closer the VGCC is to the soma, the greater influence the soma's size has on the spiking time.

Another feature that we analyzed is the voltage profiles. We consider the same models as the ones for analyzing the spiking times of the VGCCs. We consider the voltage profiles at the locations of 50, 188 and 380 μm away from the soma. This is because we would like to investigate if the simulations of the diameters size for which the calcium wave did not appear, present a similar behaviour. In Figure 3 (B)we see that for the infinite cable

and the diameter values below the critical diameter value the voltage profiles reach a higher maximum point.

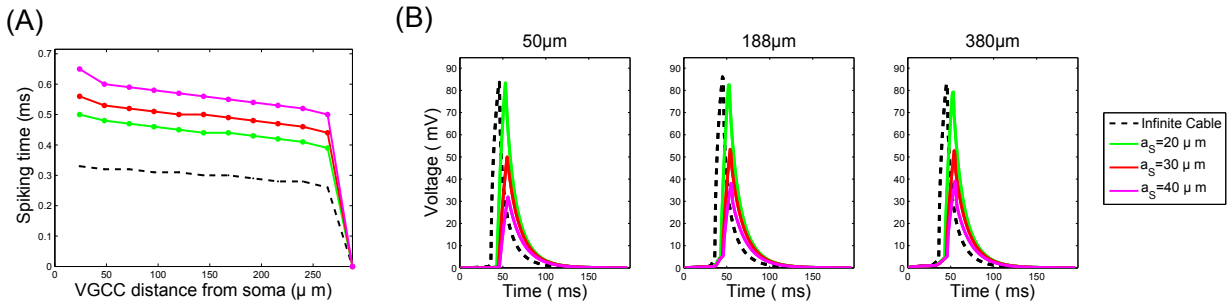

Figure 3: For the infinite cable and the semi-infinite cable model with diameters $20, 30$ and 40μm, we consider **(A)**VGCCs' Spiking times **(B)** Voltage profiles at the locations of 50, 188 and 380 μm away from the soma.

In this framework, the last feature that we analyzed is the behaviour of the RyRs, for the diameter values in which the calcium wave exists. As with the VGCCs, we recorded the firing times for the RyRs and the calcium profile in the first, middle and last RyR. We find that even as we vary the diameter, the behaviour is essentially unchanged. The difference between two firing times is of the order of .01ms. Given the last observations, we plot the results for the infinite cable and the semi-infinite cable with lumped soma with diameter $a_S = 30\mu$m. In Figure 4 (A) we see that the firing times are arranged in groups of three RyRs with brief delays in between. In Figure 4 (B) we see the different calcium profiles at distinct positions. For $a_S = 30\mu$m, the time lag the fire starts corresponds to the time that the calcium wave reaches that position. For the infinite cable, we see there is an increase of the calcium in the middle and the last RyR however it is not enough to pass the threshold and make the RyR fire.

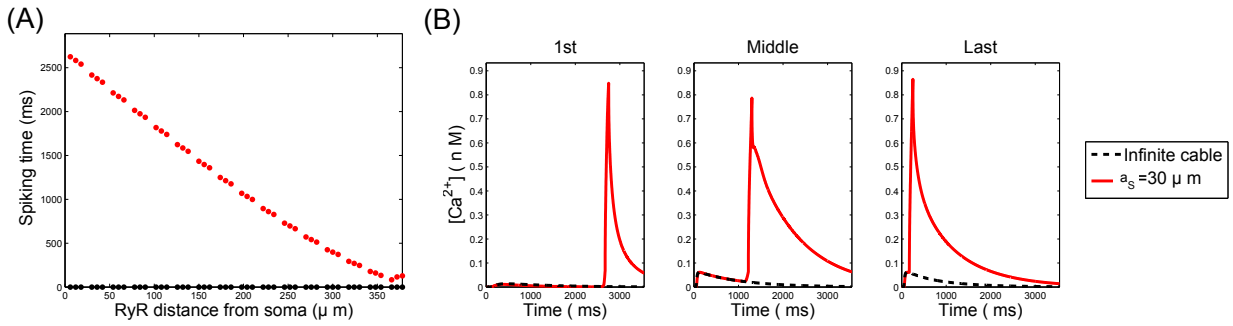

Figure 4: For the infinite cable and for semi-infinite cable with lumped soma model with diameter 30μm we have **(A)** RyR firing times **(B)** Calcium profiles for the 1st, middle and last RyR

It is important to mention that even when the graph of the firing times of the RyR seems to follow a straight line, this is not the case. In Figure 5(A), we plot the differences of firing times between each RyR and the previous one (Δ). We notice there are two distinct kinds of Δ values: Δ_1 are the differences that correspond to RyRs which are located inside the group of three RyRs between two VGCCs and Δ_2 are the differences that correspond to

RyRs between which there is a VGCC (A distribution of channels showing the two types of Δ is sketched in Figure 5 (B).

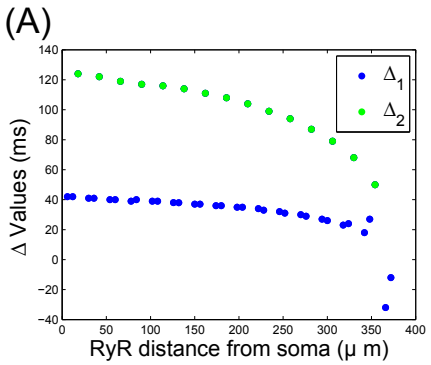

Figure 5: (A) Spiking time differences for the two types of Δ values. (B) Distribution of channels which shows which pair of RyRs corresponds to which Δ value.

Finally, we analyze one of the key factors that determine the critical diameter size. This is the distance from the soma to the initially activated VGCC. Intuitively, the farther the activation is the less effect the soma will have, so the bigger the soma will have to be in order to have an effect on the dynamics. We consider a cable 420μm long with VGCC located uniformly every 24μm and three RyRs between each pair of VGCC. For each VGCC position, we activate it as initial condition and determine the critical diameter size for which there is wave failure/wave propagation. In order to do this, we observed that for the calcium wave to enter the soma, a necessary and sufficient condition is that at least one RyR is activated, we also observed that in all the simulations the second-to-last RyR before the intially activated VGCC always activates the first. Therefore, instead of running the complete simulation to see if a calcium wave emerges, for each VGCC that we activate, we solve (for different soma's diameter sizes) the following implicit equation:

$$C(y^*, t) - h_{V_{th}} = 0$$

where y^* is the second-to-last RyR before the initially activated VGCC. If this equation does not have a solution then there is no calcium wave with the chosen soma's diameter size. This way, we determine the critical diameter size in a more computational efficent way. In Figure 6 we plot the critical diameter size against the distance from the initially activated VGCC to the soma. As expected, the a_S^* increases as the distance from the initially activated VGCC to the soma increases. An interesting feature to notice is that if the initially activated VGCC is located further away than 400μm, then there is no a_S^* and therefore no calcium wave at any diameter of the soma.

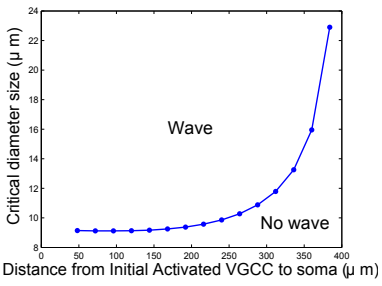

Figure 6: Critical diameter size against the distance from the initial activated VGCC to the soma. The greater this distance, the bigger the soma needs to be to have an effect.

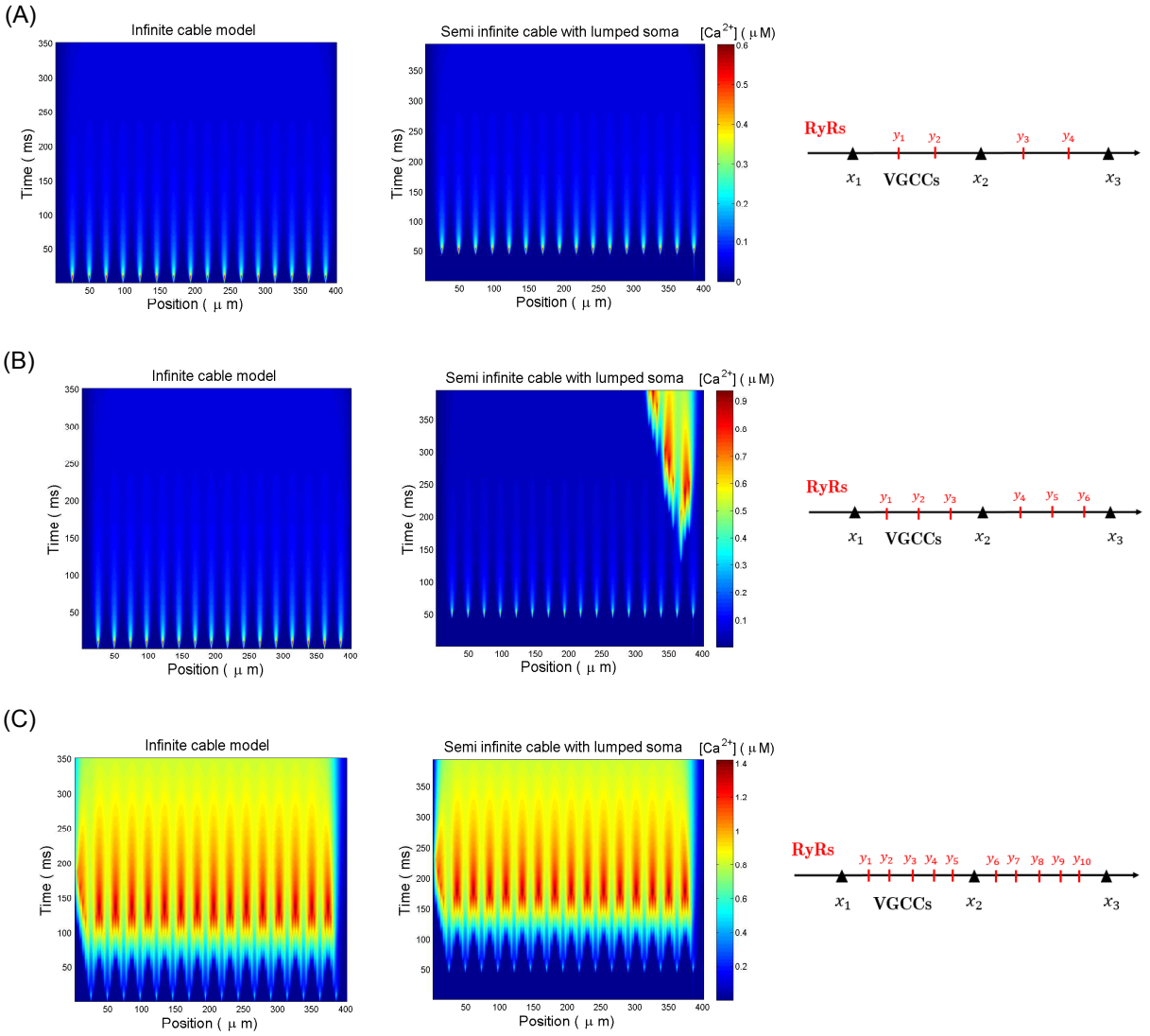

Figure 7: Calcium dynamics for both models for three different densities of the RyRs **(A)**2/24 **(B)** 3/24 and **(C)** 5/24. Simulation parameters are given in Appendix A with $a_S = 25\mu$m.

3.2 RyRs' density influence on the calcium dynamics

In this section we analyze the dependence of the calcium dynamics on the densities of the RyRs. We consider three different densities: 2/24, 3/24 and 5/24 which corresponds to 2,3 and 5 RyRs equidistantly placed between each pair of VGCCs which are located at 24μm from each other. As can be seen in Figure 7, for a density of 2/24, it is not enough to initiate and carry the wave even for the semi infinite cable with lumped soma. For a density of 3/24, the calcium waves initiates in the semi-infinite cable with the lumped soma but not in the infinite cable case. Lastly, for a density of 5/24, the density of the RyRs is sufficient to provoke a strong activation of the RyRs in both models.

4 Discussion and conclusion

In this paper, we have proposed a model to understand calcium dynamics in dendrites. We have coupled the spike-diffuse-spike model for voltage dynamics and the fire-diffuse-fire model for CICR. This model includes the effect of VGCCs in calcium dynamics and considers a discrete distributions of receptors and channels. The model leads to analytical expressions for the solution of voltage and calcium and therein lies its value. In this framework, we set out to understand how the cell geometry and the distribution of VGCCs and RyRs affect the generation and propagation of Ca^{2+} waves. Specifically, we focus on the effects of the soma's presence and size and on the effects of the RyRs' density.

For analyzing the soma's effects in calcium dynamics, we considered two models: the infinite cable model and the semi-infinite cable with lumped soma model. Taking into account realistic parameter values, we implemented the analytical solution of both models and compared their behaviour. We were particularly interested in deriving the conditions in the parameter space at which a calcium wave either propagates or does not and at which a wave may or may not enter the soma. We found that for particular values of the soma's diameter, the semi-infinite cable with lumped soma model exhibited a calcium wave whilst the infinite cable model did not. Furthermore, our results showed that there is a critical diameter value below which the calcium wave fails to exist and above which, the calcium wave initiates and reaches the soma.

To understand how the VGCCs and the RyRs affect the dynamics, we recorded their spiking and firing times and the calcium and voltage profiles for different soma diameters respectively. We found that the bigger the soma's diameter, the slower the voltage dynamics (the longer it took for the VGCCs to activate), and the smaller the highest point in the voltage profile. The behaviour below the critical diameter size and the infinite cable model was similar as expected (since there was no calcium wave in those cases). For RyRs, we saw that once we took soma's diameters size above the critical value the firing times and the calcium profiles were essentially the same.

To further understand the critical diameter size, we explored the relationship between the distance from the soma to the initially activated VGCC, and the critical diameter size a_S^*. We saw that for the calcium to enter the soma a necessary and sufficient condition is that at least one RyR is activated. This simplifies the determination of a_S^* since instead of running a simulation to see if a calcium wave emerges, we just solve an implicit equation for the third-to-last RyR.

Our study raises a number of questions. Since the solutions are explicitly expressed, is there an analytical framework that would allow us to determine the critical diameter size without solving implicit equation? Is there a critical distance and density for the RyRs to support a calcium wave? The spiking differences for the RyRs follow a distinct pattern, is there an analytical function that could give us that pattern? Finally, why is the third RyR the one who fires the first?

The analysis we developed in this paper provides a framework for the investigation of calcium waves in dendrites. One natural extension of this work is to consider more realistic dendritic structures. This has previously been considered for voltage in [19]. In our case, as

we already mention, the PDE (2) can be defined in any network structure. To get a solution for this system of PDEs, one can consider the sum-over-trips approach that defines the Green function of an arbitrary network structure [1]. It is important to notice that in our case we were able to derive an analytical expression for the solution of the PDE. However in most of the cases this is not possible and one needs to perform an inverse laplace transform numerically.

A further extension would be to consider a simplified structure with a branching point. Experimentally, Ca^{2+} waves preferentially initiate at branch points in the dendrites of pyramidal neurons, even when the stimulating electrode is not directly opposite to the branch point [12]. Studying a branching structure can provide an insight for this experimentally observed fact.

There are several features that one could include in our model to make it more realistic: First, the fire-diffuse-fire lacks any notion of a recovery variable which makes it unsuitable for general application. There are also other sources of Ca^{2+} that we need to take into account: IP_3, action potentials and synaptic potentials [15]. Also, there is a feedback dynamics in calcium dynamics that we are ignoring: cytoplasmic buffers and pumps that return Ca^{2+} to resting levels. Moreover, there is a feedback dynamics relating calcium and voltage given by the presence of Ca^{2+} activated K channels. However this is still a good model to work with; in [18] the authors prove that the spike-diffuse-spike model provides good results comparing to more realistic models. In addition, the model can be modified to include a refractory term in the spiking and firing events and study multiple spiking times from the same site.

In conclusion, our findings give an insight for the soma's influence in calcium dynamics when we take into account the voltage. Furthermore, the analysis for the different RyRs' densities help us understand the role of the distribution of RyRs in calcium dynamics.

Acknowledgments

I would like to thank my supervisor Yulia Timofeeva for her support, her patience, interesting discussions and valuable suggestions throughout this project. I also would like to thank Janis Klaise for proofreading this work. Finally, I would like to thank Erasmus Mundus for the funding, and the Centre for Complexity Science for providing an engaging working environment.

References

1. Abbott L.F., Farhi E, Gutmann S.: The path integral for dendritic trees. Biol Cybern. **66**(1), 49-60 (1991)

2. Abramowitz, Milton, Stegun, Irene A.: Handbook of Mathematical Functions with Formulas, Graphs, and Mathematical Tables, New York: Dover Publications,(1972)

3. Berridge, M., Lipp, P., & Bootman, M.: The versatility and universality of calcium signalling. Nature Reviews. Molecular Cell Biology, **1**(1), 11-21(2000)

4. Berridge, M. J., Bootman, M. D. & Roderick, H. L.: Calcium signalling: dynamics, homeostasis and remodelling. Nature Rev. Mol. Cell Biol. **4**(7): 517–529 (2003)

5. Coombes, S and Bressloff, P C: Solitary waves in a model of dendritic cable with active spines, SIAM J Appl Math, **61** 432-453 (2000)

6. Coombes,S: The effect of ion pumps on the speed of travelling waves in the fire-diffuse-fire model of Ca^{2+} release. Bulletin of Mathematical Biology **63**, 1-20 (2001)

7. Coombes, S & Bressloff, P. C. Saltatory waves in the spike-diffuse-spike model of active dendritic spines, Physical Review Letters. **91** (2003)

8. Hagenston, A. M., Fitzpatrick, J. S. & Yeckel, M. F. MGluR-mediated calcium waves that invade the soma regulate firing in layer V medial prefrontal cortical pyramidal neurons. Cereb. Cortex 18, 407–423 (2008).

9. Keizer, J., et al. Saltatory propagation of Ca2+ waves by Ca2+ sparks. Biophys. J. **75** 595–600 (1998)

10. Luo, D. et al. Nuclear Ca2+ sparks and waves mediated by inositol 1,4,5-trisphosphate receptors in neonatal rat cardiomyocytes. Cell Calcium **43**, 165–174 (2008)

11. Martone, M., Zhang, Y., Simpliciano, V., Carragher, B. & Ellisman, M. Three-dimensional visualization of the smooth endoplasmic reticulum in Purkinje cell dendrites. J. Neurosci. **13**, 4636–4646 (1993)

12. Nakamura, T., Lasser-Ross, N., Nakamura, K. & Ross, W. N. Spatial segregation and interaction of calcium signalling mechanisms in rat hippocampal CA1 pyramidal neurons. J. Physiol. **543**, 465–480 (2002)

13. Peercy BE., Initiation and propagation of a neuronal intracellular calcium wave. J Comput Neurosci. **2**, 334-48 (2008)

14. Power, J. M. & Sah, P. Nuclear calcium signalling evoked by cholinergic stimulation in hippocampal CA1 pyramidal neurons. J. Neurosci. **22**, 3454–3462 (2002)

15. Ross WN. Understanding calcium waves and sparks in central neurons. Nat Rev Neurosci. **13**(3):157-68 (2012)

16. Sneyd, J., Keizer, J., & Sanderson, M.: Mechanisms of calcium oscillations and waves: a quantitative analysis. FASEB Journal: Official Publication Of The Federation Of American Societies For Experimental Biology, **9**(14), 1463-1472(1995)

17. Spacek, J. & Harris, K. M. Three-dimensional organization of smooth endoplasmic reticulum in hippocampal CA1 dendrites and dendritic spines of the immature and mature rat. J. Neurosci. **17**, 190–203 (1997)

18. Timofeeva Y, Lord G J & Coombes S: Spatio-temporal filtering properties of a dendritic cable with active spines, Journal of Computational Neuroscience, **21**, 293-306 (2006)

19. Timofeeva, Y, Coombes, S, Michieletto, D: Gap junctions, dendrites and resonances: a recipe for tuning network dynamics, Journal of Mathematical Neuroscience, **3**(15) (2013)

20. Tuckwell, Henry C. Introduction to Theoretical Neurobiology, Volume 1. Linear Cable Theory and Dendritic Structure. Cambridge University Press, 1988.

21. Parker I & Yao Y . Regenerative release of calcium from functionally discrete subcellular stores by inositol trisphosphate. Proceedings of the Royal Society London B, **246**:269–274 (1991)

22. M Yamakage , A Namiki. "Calcium channels — basic aspects of their structure, function and gene encoding; anesthetic action on the channels — a review". Can J Anaesth **49**(2):151–64 (2002)

A Appendix A: Simulation parameters

Neuron parameters	Voltage parameters	Calcium parameters
a=2 μ m	$D_V = 5 \times 10^4 \mu m^2/ms$	$D_C = 0.023 \mu m^2/ms$
μ m	$\tau_V = 2$ms	$\tau_C = 100$ ms
$C_m = 1$ μF/cm^2		$\gamma = 6^{-5}$ μ M / mV
$R_a = 100$ Ω m	Distance between each VGCC=24 μ m	RyR between VGCC=3
$g_m = 0.5 \times 10^{-3}$S/cm^2	$\tau_{VGCC} = 1$ ms	$\tau_{RyR} = 8$ ms
	$\sigma_{VGCC} = 2705.63403$ m V μ m	$\sigma_{RyR} = 0.06$ m V μm
	$h_{VGCC} = 1$ mV	$h_ryr = 0.0616525$ nM
Total time=80 ms Total length=400 μ m, dt_V=0.01, dt=dx=0.1, Initial vgcc active =3		